Influence of Hydrogen Bonding on the Crystallization Behavior of Semicrystalline Polyurethanes

Robin L. McKiernan, Amy M. Heintz, Shaw L. Hsu, Edward D. T. Atkins,† Jacques Penelle, and Samuel P. Gido*

Department of Polymer Science and Engineering, University of Massachusetts, Amherst, Massachusetts 01003-4530

Received January 25, 2002; Revised Manuscript Received May 31, 2002

ABSTRACT: A series of linear, aliphatic *m*,*n*-polyurethanes $[O-(CH_2)_m-O-C(O)-NH-(CH_2)_n-NH-C(O)]_x$ derived from long-chain aliphatic diols $HO-(CH_2)_m-OH$, where $m = 12$, 22, or 32, and much shorter diisocyanates $O=C=N-(CH_2)_n-N=C=O$, where $n = 4$, 6, 8, or 12, were previously characterized and shown to have physical and thermal properties similar to polyethylene. The current study shows, however, that hydrogen bonding still exercises a controlling influence on the crystallization process of these long-chain, aliphatic polyurethanes. X-ray diffraction, electron diffraction, and infrared spectroscopy indicate that these long alkane segment polyurethanes have interchain and intersheet distances similar to that seen for polyamides and polyurethanes of higher hydrogen bonding densities. Hydrogen bonding controls the crystallization, packing, and morphology of these polyurethanes, resulting in a crystal structure analogous to that of aliphatic, even−even (syncephlic) polyamides and unlike that of polyethylene. Additionally, high-temperature infrared studies show the existence and high concentration (∼75%) of hydrogen bonding in these polyurethanes even in the melt.

Introduction

Typical aliphatic *m*,*n*-polyurethanes $[O-(CH_2)_m-O-C(O)-NH-(CH_2)_n-NH-C(O)]_x$, where *m* and *n* represent the number of uninterrupted methylene groups originating from the diol and diisocyanate, respectively, have crystal structures similar to the corresponding aliphatic polyamides (triclinic or monoclinic, depending on whether *m* and *n* are even or odd and on their length, and a varying amount of pseudohexagonal phase).[1−5] Their all-trans chains are oriented parallel to each other in order to maximize the contribution of the hydrogen bonds C=O···H−N between neighboring stems to the overall stability of the crystal structure (Figure 1a). In contrast, linear polyethylene also has an all-trans conformation, but with no hydrogen-bonding groups in the aliphatic backbone crystallize by packing into an orthorhombic unit cell in order to maximize the van der Waals bonds between the chains (Figure 1b).

By increasing the length of the aliphatic segments of the *m*,*n*-polyurethanes, the influence of the carbamate esters O−C(O)−NH is progressively diluted. The physical and thermal characteristics (e.g., solubility, melting temperature, and enthalpy) of a series of increasingly aliphatic polyurethanes have been previously shown to resemble linear high-density polyethylene (HDPE).[6] It can reasonably be expected that above a certain methylene/carbamate ester ratio the crystallization behavior (e.g., crystal structure, morphology, lamellar thickness, annealing behavior, and kinetics) of these aliphatic polyurethanes will approach that of linear polyethylene.

In this present study, it was desired to establish whether the onset of the transition from a polyurethane- or polyamide-like to a polyethylene-like behavior occurred and, if so, to investigate the details of the crystallization process at and close to that transition region. A better understanding of the balance between methylene−methylene van der Waals interactions and hydrogen bonding in semicrystalline polymer structures is expected to be extremely useful in the design of self-assembling polymers and aid in the engineering and fine-tuning of the crystallinity of these systems.

Experimental Section

Polymer Synthesis. The aliphatic *m*,*n*-polyurethanes discussed in this paper had the general structure $[O-(CH_2)_m-O-C(O)-NH-(CH_2)_n-NH-C(O)]_x$. The increasingly aliphatic series consisted of 12,4; 12,6; 12,8; 12,12; 22,4; 22,6; 22,8; 22,-12; 32,4; 32,6; 32,8; and 32,12. The synthesis of all these *m*,*n*-polyurethanes from long-chain α,ω-diols and much shorter α,ω-diisocyanates was described previously.[6]

Sample Preparation. Melt-crystallized samples were prepared by heating the polymers to 200 °C and then allowing the polymers to cool to room temperature at a rate of 10 K min^{-1}. Solution-grown crystals were prepared from 0.01% w/v solutions of the polymers in *N*,*N*-dimethylformamide (DMF). The mixtures were heated until the polymers dissolved, and once dissolved, the samples were rapidly cooled to room temperature, slowly reheated to the temperature where the polymers dissolved, cooled to the crystallization temperature, and then held at this temperature for several days. Oriented mats suitable for X-ray diffraction were prepared by draining the crystal suspension through a 0.22 μm filter.

X-ray Diffraction. Small-angle X-ray scattering (SAXS) experiments were obtained at room temperature using Ni-filtered Cu Kα radiation of wavelength 1.542 Å from a Rigaku rotating anode operating at 40 kV and 200 mA. A point-collimated 300 μm diameter beam was used, and the X-ray scattering patterns were recorded using an evacuated Siemens GADDS two-dimensional area detector. Wide-angle X-ray scattering (WAXS) experiments were obtained at room temperature using Ni-filtered Cu Kα radiation of wavelength 1.542 Å from a Siemens sealed tube X-ray generator operating at 40 kV and 30 mA. A point-collimated beam was used, and the X-ray scattering patterns were recorded using a flat image plate in an evacuated Statton camera. Calcite ($d_b = 3.035$ Å) was dusted onto selected samples for calibration purposes.

† Visiting professor. Permanent address: H. H. Wills Physics Laboratory, University of Bristol, Tyndall Avenue, Bristol, BS8 1TL U.K.

* Corresponding author: Fax +1-413-545-0082; e-mail spgido@squeaky.pse.umass.edu.

10.1021/ma0201274 CCC: $22.00
Published on Web 08/02/2002

Table 1. SAXS and WAXS Results

m,*n*-polymer	LSP (Å)	d_{100} (Å)	d_{200} (Å)	d_{010} (Å)	first-order d_{001} (Å)	second-order d_{001} (Å)	third-order d_{001} (Å)	theor repeat distance (Å)	tilt angle (deg)
12,4	104	4.6	4.1	3.8	20.4			27	41
12,6	108	4.7	4.1	3.7	21.0	10.5	7.0	29.5	45
12,8	119	4.5	4.1	3.7	24.4	12.2		32	40
12,12	134	4.3		3.7		13.8		37	42
22,4	149	4.6	4.1	3.8			11.3	39.5	31
22,6	102	4.6	4.1	3.7			11.0	42	38
22,8	136	4.6	4.1	3.7		17.3	11.5	44.5	39
22,12	139	4.5	4.2	3.8	36.0	18.0	12.0	49.5	43
32,4	182	4.5	4.1	3.7					
32,6	137	4.5	4.1	3.7					
32,8	130	4.5	4.1	3.7					
32,12	131	4.5	4.1	3.7					

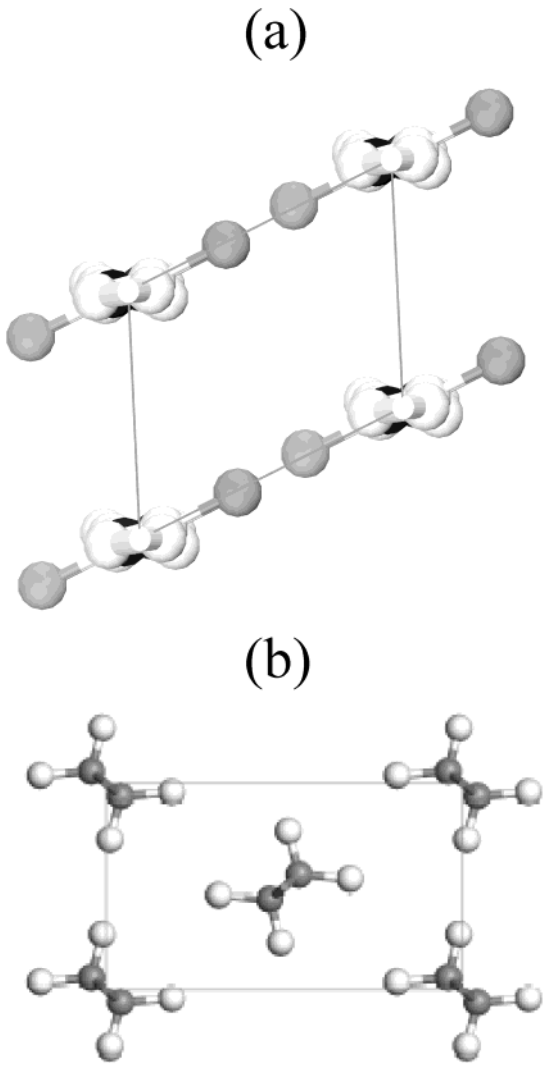

Figure 1. Projection, parallel to the chain *c*-axis, of crystal structure: (a) typical triclinic polyurethanes/polyamides and (b) room temperature, orthorhombic polyethylene.

SAXS and WAXS experiments were also performed on the Advanced Polymers Beamline (X27C) at the National Synchrotron Light Source, Brookhaven National Laboratory, Upton, NY. The small- and wide-angle camera lengths were calibrated using an Ag-B_0 standard and calcite, respectively. The X-ray beam had a 3 mm^2 area and a wavelength of 1.307 Å. Custom software was used to subtract the background, circularly average the data, and convert the data to a logarithmic intensity scale.

Electron Microscopy. Carbon-coated transmission electron microscope (TEM) grids were dipped into the 0.01% w/v crystal suspensions, and the solvent was allowed to evaporate in a vacuum oven at room temperature. Some samples were shadowed with Pd−Pt to enhance the contrast of the TEM images. To differentiate the crystalline and amorphous regions of the polymers, melt-crystallized polymers were stained using a 2% solution of ruthenium(III) chloride hydrate in sodium hypochlorite. The ruthenium oxide-stained samples were then microtomed at room temperature into 40 nm slices using a Leica ULTRACUT UCT universal ultramicrotome. The microtomed samples were deposited onto copper grids and dried in a vacuum oven at room temperature. The magnification was calibrated using a crossed lined grated replica with 2160 lines/mm. TEM images were recorded at room temperature using a JEOL 100 CX microscope operating at 100 kV.

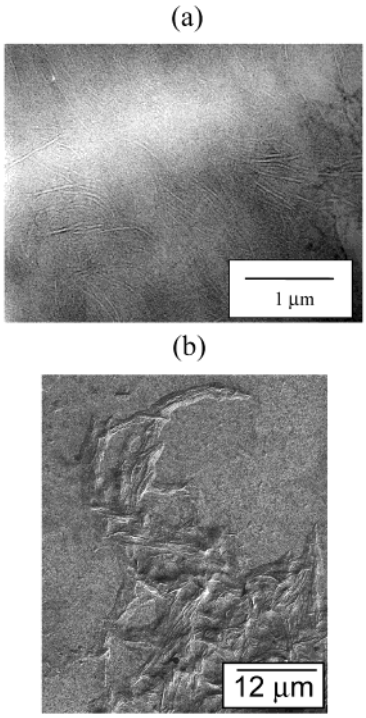

Figure 2. TEM images: (a) melt-crystallized 22,6-polyurethane lamellae (amorphous regions are black and crystalline regions are white) stained with RuO_4 and (b) solution-grown 22,12-polyurethane coated with Pd−Pt to increase the contrast.

Spectroscopy. A Bruker FRA 106 spectrometer equipped with a Nd:YAG laser (1.064 μm) was used to record the Fourier transform Raman (FT Raman) spectra. A total of 256 scans were performed, and spectral resolution was 4 cm^{-1}. The laser power was 150 mW, and the excitation/collection geometry was 180°. The polyurethanes were examined in the bulk without any special crystallization treatment.

Fourier transform infrared (FTIR) spectra were recorded on either a Bio-Rad FTS 175C spectrometer at room temperature or a Perkin-Elmer Spectrum 2000 system with a wide-band MCT detector at elevated temperatures. A home-built heating

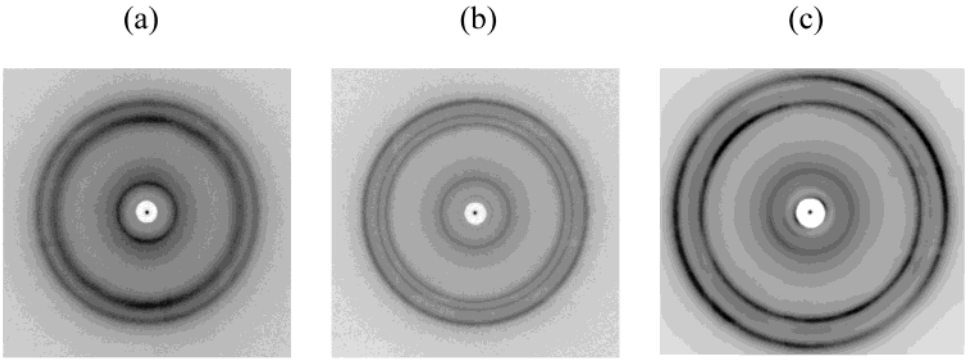

Figure 3. WAXS patterns: (a) melt-crystallized 12,12-polyurethane; (b) melt-crystallized 12,8-polyurethane; and (c) solution-grown 22,12-polyurethane; mat normal direction 45° clockwise from vertical.

cell attached to an Omega proportioning temperature controller with an accuracy of 2 °C was employed to control the temperature of the infrared cell. The temperature was calibrated to the melting point of benzoic acid. A total of 16 scans were performed, and spectral resolution was 4 cm^{-1}. Analysis of the data was performed using Spectrum 2000 software, and literature procedures[7] were used to deconvolute the amide I region of the spectra. Pellets were prepared by grinding a small amount of polymer with KBr and then pressing the mixture into pellets. Films were prepared by dissolving the polymer in hot *o*-dichlorobenzene and then casting a film onto KBr plates. The resulting polymer films were approximately 5−10 μm thick.

Results and Discussion

Lamellar Thickness. The lamellar thickness of the melt-crystallized polyurethanes was determined using SAXS (Table 1). Aliphatic polyurethanes and polyamides of high hydrogen-bonding density typically have lamellar stacking periodicities (LSPs) in the range 60−80 Å.[8] However, the polyurethanes in this study with their longer aliphatic segments showed LSP values more typical of polyethylene (110−140 Å).[9]

TEM imaging was used to examine the ruthenium oxide-stained, melt-crystallized 22,*n*-polyurethanes. The stain preferentially penetrated the amorphous regions and allowed for the visualization of the lamellar morphology. The experimental LSP values determined using TEM were consistent with that found using SAXS. Figure 2a shows the TEM image of the lamellae of the 22,6-polyurethane, which is representative of that seen for the other polyurethanes in this series. TEM imaging at 20 000 times magnification showed that the solution-grown polymers all formed extended aggregates of overlaying lathlike lamellae (Figure 2b) similar to those formed by polyamides under similar experimental conditions.[1]

Crystal Structure. Several studies have shown that polyurethanes have a similar crystal structure as their corresponding polyamides.[1−5] However, the polyurethanes in this study contain substantially longer alkane segments. The lower density of hydrogen bonding in these polyurethanes resulted in an alteration in the thermal and physical properties toward that of HDPE.[6] If hydrogen bonding was the controlling crystallization factor, a diffraction pattern similar to that of aliphatic polyamides should be seen. Single-chain, triclinic polyamides are characterized by two strong WAXS diffraction peaks at *d*-spacings of 4.4 Å (d_{100}) and 3.7 Å (d_{010} and d_{110}).[10] Depending on their crystallization temperature, particularly if they are quenched from the melt, some high-temperature pseudohexagonal packing can occur

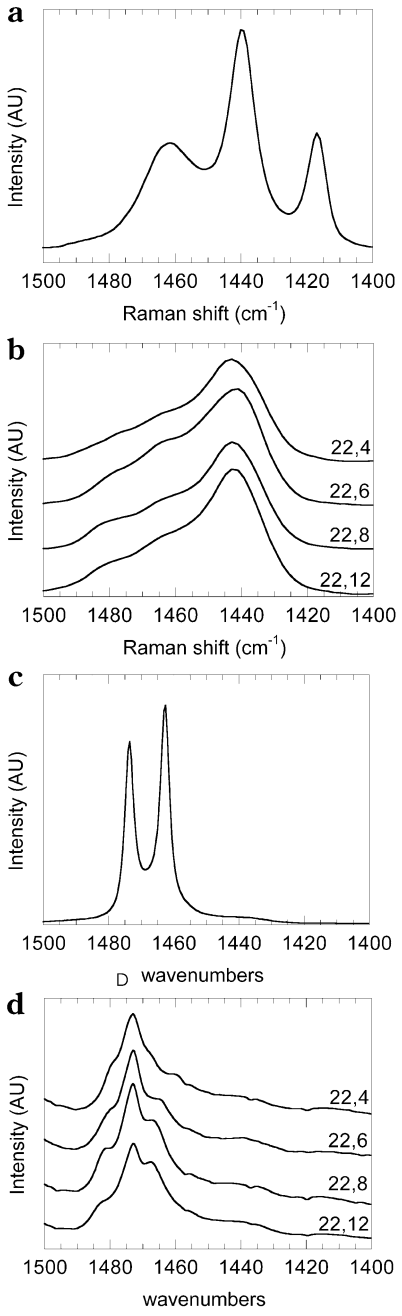

Figure 4. CH_2 bending region: (a) Raman spectrum of polyethylene; (b) Raman spectra of 22,*n*-polyurethanes; (c) IR spectrum of polyethylene; and (d) IR spectra of 22,*n*-polyurethanes.

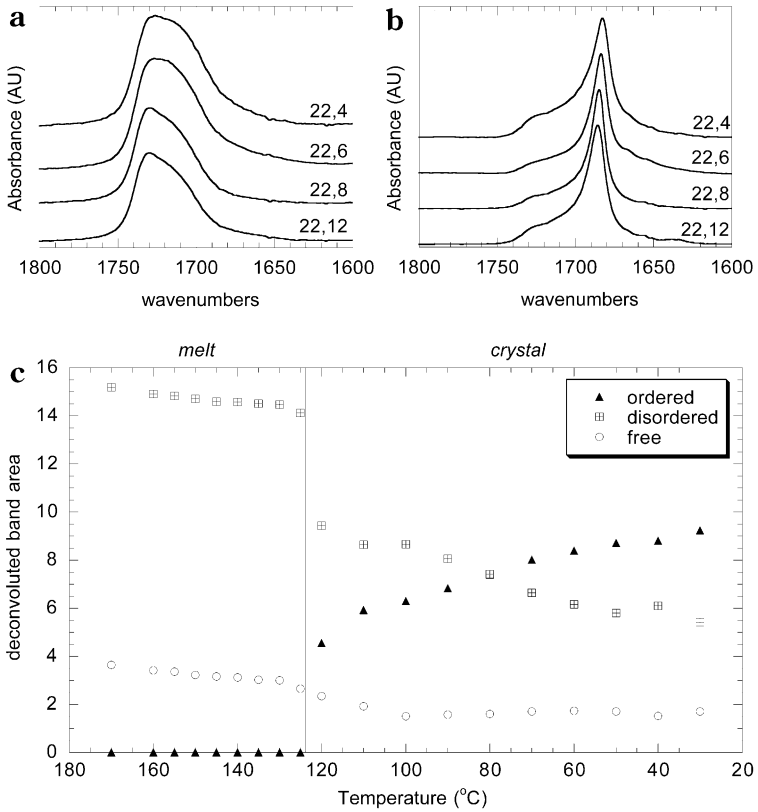

Figure 5. (a) IR spectra (amide I region) of 22,*n*-polyurethanes in the melt; (b) IR spectra (amide I region) of melt-crystallized 22,*n*-polyurethanes; and (c) evolution of ordered hydrogen bonding during the crystallization of 22,12-polyurethane.

and is characterized by a WAXS diffraction peak at a *d*-spacing of 4.2 Å (d_{200}).[11] However, if the alkane segments of the *m*,*n*-polyurethanes are sufficiently long, the energy from the van der Waals forces, ~1 kJ mol^{-1}, might overcome the energy gained from hydrogen bonding, 10−40 kJ mol^{-1}, resulting in a crystallization that mimics polyethylene. The orthorhombic polyethylene phase exhibits WAXS diffraction peaks at *d*-spacings of 4.1 Å (d_{110}) and 3.7 (d_{200}).[12]

The WAXS patterns of this family of *m*,*n*-polyurethanes were all similar regardless of the length of the aliphatic segments with the exception of the melt-crystallized 12,12-polyurethane (Figure 3a), which, for reasons not fully understood, has only two observable diffraction rings. The diffraction patterns obtained from powdered mats (Figure 3b) or taken with the incident X-ray beam orthogonal to the mat surface (Figure 3c) exhibited the same diffraction features and measured *d*-spacings; thus, the lamellae obtained by crystallizing from the melt and isothermally from solution were the same. There was no preferred orientation, and the Bragg diffraction signals therefore appeared as rings.

The *m*,*n*-polyurethanes exhibit strong intensity at a *d*-spacing of 4.7−4.5 Å and 3.8−3.7 Å (Table 1). A weaker diffraction peak at a *d*-spacing of 4.2−4.1 Å is sometimes observed, the relative intensity of which is a function of the crystallization conditions. The *d*-spacings of the two prominent diffraction peaks appear to be related to the characteristic 4.4 Å (d_{100}) and 3.7 Å (d_{010}) typically seen for even−even polyamides in the usual triclinic crystal phase,[11] the differences suggesting different values of shearing in the triclinic unit cell. This is to be discussed in a more detailed structural analysis.[13] A weaker diffraction peak at a *d*-spacing of 4.1−4.2 Å has also been observed in even−even nylons, e.g. ref 14, and is thought to emanate from a pseudohexagonal phase.

Some of the polymers also displayed diffraction peaks, with varying intensities within the polyurethane family, with a *d*-spacing range of 7.0−36.0 Å (see Figure 3a−c). These spacings are orders of the fundamental structural repeat (d_{001}). Thus, the angle of the chain tilt with respect to the lamellar surface ($c \wedge c^*$) can be estimated from these d_{001}-spacings using the following expression

$$\text{tilt angle} = \cos^{-1}(\text{observed } d_{001}/\text{theoretical repeat length}) \quad (1)$$

At this level of analysis, an all-trans conformation for the chain was taken. Clearly, perturbations from the all-trans conformation will increase the tilt angle slightly. The tilt angles calculated using eq 1, and the WAXS data are given in Table 1 and range from 31° to 45°. The values bear a relationship to the value ~42° observed for nylon-6,6.[14]

Attempts to obtain oriented samples proved unsuccessful for all but the 22,12-polyurethane. These attempts included pulling and stretching fibers, trying to orient thin polymer films made from the melt, and making single crystal mats from a variety of solvents. This was probably the result of the low percent crystallinity of the polyurethanes.[15] In the case of the solution-grown 22,12-polyurethane, sedimented mats were obtained that exhibited partial orientation as can be seen in the X-ray diffraction pattern shown in Figure 3c. It was judged that these data were of sufficient quality to warrant a more detailed analysis of the crystalline structure of the 22,12-polyurethane, including the unit cell parameters, chain conformation, and packing; these results will be discussed in another paper.[13]

Further confirmation that the *m*,*n*-polyurethanes, regardless of their low hydrogen-bonding density, did not have an orthorhombic crystal structure similar to polyethylene came from the Raman and IR spectra. The Raman spectra of orthorhombic polyethylene (Figure 4a) and monoclinic *n*-paraffins exhibit bands (CH_2 bend) at 1418, 1441, and 1463 cm^{-1} and at 1418, 1441, and 1462 cm^{-1}, respectively.[16] However, the Raman spectra of the *m*,*n*-polyurethanes did not exhibit the band at 1418 cm^{-1} (Figure 4b). Their Raman spectra were similar to that of triclinic and hexagonal *n*-paraffins with bands at 1445, 1463, and 1484 cm^{-1} and at 1438 and 1458 cm^{-1}, respectively.[16]

Unlike the orthorhombic polyethylene phase (Figure 4c), the *m*,*n*-polyurethanes (Figure 4d) did not display the typical Davydov splittings at 720−730 cm^{-1} (CH_2 rock) and 1460−1470 cm^{-1} (CH_2 bend) seen for orthorhombic polyethylene[17] and long-chain *n*-paraffins.[18] As previously reported,[15] the energy gained from hydrogen bonding for the 22,8-polyurethane was determined by IR to be 11.47 kJ (mol per urethane)$^{-1}$ or 22.93 kJ (mol per repeat)$^{-1}$. Therefore, hydrogen bonding was still able to compete with the energy that would be gained from the van der Waals forces of 22 consecutive methylene groups packed in an orthorhombic unit cell, resulting in the triclinic packing of the *m*,*n*-polyurethanes.

High-Temperature Studies. To determine when and how much hydrogen bonding occurred during the crystallization process, the amide I region of the 22,*n*-polyurethanes was examined using high-temperature IR spectroscopy. The amide band is associated with a distribution of distances and geometries of hydrogen bonds.[15,19−21] Two extremes are easy to characterize. At one extreme is the hydrogen-bonded carbonyl groups (1684 cm^{-1}) with ordered geometry such as the one in the crystalline state. The other extreme is the free carbonyl group (1732 cm^{-1}). However, disordered hydrogen-bonded carbonyl groups (1704 cm^{-1}) are also formed.[7] The IR spectra showed the existence of hydrogen bonds in the melt (Figure 5a) and the ordering of these bonds upon crystallization (Figure 5b). The melt consisted of highly interacting chains and was more than 75% hydrogen-bonded (Figure 5c). This might explain why the melting temperatures of the increasingly aliphatic *m*,*n*-polyurethanes approached that of polyethylene.[6] Since the polymers could still contain hydrogen bonds in the melt, the polyurethanes needed only enough heat to break up the crystalline alkane segments of the polymers in order to melt. The increasing solubility of these polyurethanes in solvents used for HDPE like *o*-dichlorobenzene and decreasing solubility in solvents typically used for polyamides like *m*-cresol and DMF[6] might be the result of a similar presence of hydrogen bonds even in solution.

Conclusions

Previous work showed that polyethylene-like polyurethanes could be synthesized by diluting the amount of carbamate esters.[6] Increasing the length of the aliphatic segments of the polymers resulted in changing the physical and thermal characteristics (e.g., solubility, melting point, enthalpy, and lamellar thickness) from that typical of polyurethanes and polyamides toward that of polyethylene. However, X-ray, electron microscopy, and IR spectroscopy have all shown that hydrogen bonding still controlled the crystallization process of these *m*,*n*-polyurethanes. The result was that these long-chain aliphatic polyurethanes had the analogous crystal structure (triclinic and a varying amount of pseudohexagonal) and crystallization behavior as polyamides and polyurethanes of higher hydrogen-bonding densities. The results clearly showed that a transition from polyamide-like to polyethylene-like was not encountered, even for the 32,12-polyurethane. Thus, the aliphatic segments of this series of polyurethanes will need to be further increased if such a transition is to be discovered. Interestingly, a similar pattern of behavior, where interchain hydrogen bonding has a dominant role, has recently been found for long alkane, even−even nylons.[22]

Acknowledgment. This work is supported by NSF Material Research Science and Engineering Center (MRSEC) (NSF Grant DMR-9809365). E.D.T.A. thanks the Engineering and Physical Science Research Council (UK) for support. The use of MRSEC central experimental facilities and W. M. Keck Polymer Morphology Laboratory at the University of Massachusetts is acknowledged, as is the use of the Advanced Polymers Beamline of the National Synchrotron Light Source at the Brookhaven National Laboratory.

References and Notes

(1) Dreyfuss, P.; Keller, A. *J. Macromol. Sci., Phys.* **1970**, *4*, 811.
(2) Saito, Y.; Nansai, S.; Kinoshita, S. *Polym. J. (Tokyo)* **1972**, *3*, 113.
(3) Blackwell, J.; Gardner, K. H. *Polymer* **1979**, *20*, 13.
(4) Blackwell, J.; Ross, M. *J. Polym. Sci., Polym. Lett. Ed.* **1979**, *17*, 447.
(5) Saito, Y.; Hara, K.; Kinoshita, S. *Polym. J. (Tokyo)* **1982**, *14*, 19.
(6) McKiernan, R. L.; Gido, S. P.; Penelle, J. *Polymer* **2002**, *43*, 3007.
(7) Coleman, M. M.; Lee, K. H.; Shrovanek, D. J.; Painter, P. C. *Macromolecules* **1986**, *19*, 2149.
(8) Keller, A. *Philos. Mag.* **1957**, *2*, 1171. Geil, P. H. *Polymer Single Crystals*; Interscience: New York, 1963. Keller, A. *Prog. Phys.* **1968**, *31*, 41.
(9) Seto, T.; Hara, T.; Tanaka, T. *Jpn. J. Appl. Phys.* **1968**, *7*, 31.
(10) Bunn, C. W.; Alcock, T. C. *Trans. Faraday Soc.* **1945**, *41*, 317.
(11) Bunn, C. W.; Garner, E. V. *Proc. R. Soc. London, Part A* **1947**, *189*, 39.
(12) Bunn, C. W. *Trans. Faraday Soc.* **1939**, *35*, 482.
(13) McKiernan, R. L.; Sikorski, P.; Atkins, E. D. T.; Gido, S. P.; Penelle, J. *Macromolecules* **2002**, in press.
(14) Jones, N. A.; Atkins, E. D. T.; Hill, M. J.; Cooper, S. J.; Franco, L. *Macromolecules* **1996**, *29*, 6011.
(15) Heintz, A. M.; McKiernan, R. L.; Gido, S. P.; Penelle, J.; Hsu, S. L. *Macromolecules* **2002**, *35*, 3117.
(16) Boerio, F. J.; Koenig, J. L. *J. Chem. Phys.* **1970**, *52*, 3425.
(17) Bower, D. I.; Maddams, W. F. *The Vibrational Spectroscopy of Polymers*; Cambridge University: Cambridge, 1989.
(18) Lee, K.-S.; Wagner, G.; Hsu, S. L. *Polymer* **1987**, *28*, 889.
(19) Lee, H. S.; Wang, Y. K.; Hsu, S. L. *Macromolecules* **1987**, *20*, 2089.
(20) Lee, H. S.; Wang, Y. K.; MacKnight, W. J.; Hsu, S. L. *Macromolecules* **1988**, *21*, 270.
(21) Lee, H. S.; Hsu, S. L. *Macromolecules* **1989**, *22*, 1100.
(22) Ehrenstein, M.; Sikorski, P.; Atkins, E. D. T.; Smith, P. *J. Polym. Sci., Part B, Polym. Phys.* **2002**, in press.

MA0201274